

Stability of Hybrid-Wing–Body-Type Aircraft with Centerbody Leading-Edge Carving

M. A. Sargeant,^{*} T. P. Hynes,[†] and W. R. Graham[‡]

University of Cambridge, Cambridge, England CB2 1PZ, United Kingdom
and

J. I. Hileman,[§] M. Drela,^{||} and Z. S. Spakovszky^{**}

Massachusetts Institute of Technology, Cambridge, Massachusetts 02139

DOI: 10.2514/1.46544

The silent-aircraft experimental aircraft are balanced by generating lift near the aircraft nose through leading-edge carving of the centerbody. The use of leading-edge carving over the centerbody is novel, in that previous blended-wing–body aircraft have balanced the aircraft by downloading the centerbody (via reflex camber) to achieve the effect of a tail. This paper decomposes the aerodynamic forces into contributions from spanwise sections to explain how three-dimensional flow effects are beneficial in allowing the silent-aircraft experimental aircraft to be both statically stable and to have an elliptical lift distribution over a large range of angles of attack. By analyzing the results in this manner, rationale is also given as to why, unlike other blended-wing–body-type configurations, the silent-aircraft-experimental design can use supercritical unstable-outer-wing airfoil profiles to generate a balanced and stable aircraft. The results are then used to develop a methodology to aid the aircraft designer in determining the amount of leading-edge carving that is necessary to achieve static stability for blended-wing–body-type aircraft.

Nomenclature

b	=	span (location where winglet attaches to main wing), m
C_m	=	moment coefficient
c	=	local chord length
c_l	=	local lift coefficient
c_{ref}	=	reference chord length (mean chord)
t/c	=	thickness/chord
x_{ac}	=	airfoil aerodynamic center, measured relative to the aircraft nose
x_{cg}	=	aircraft center of gravity location, measured relative to the aircraft nose
x_{cp}	=	airfoil center of pressure, measured relative to the aircraft nose
y	=	y coordinate (spanwise), m
α	=	angle of attack, deg
α_d	=	induced angle from downwash
α_{nolift}	=	zero lift angle

I. Introduction

THE Cambridge–MIT Institute’s Silent Aircraft Initiative (SAI) was launched in November 2003 and culminated in the design of the silent aircraft experimental (SAX) version 40 (SAX-40) in November 2006. In addition to providing a step change in noise emissions, the conceptual aircraft design is predicted to be aerodynamically efficient, with a fuel economy that is potentially 25% better than current aircraft designs (Hileman et al. [1]) Although

the blended-wing–body (BWB) planform used in the SAX-40 may look similar to past BWB designs (including Liebeck [2] and Qin et al. [3]), the use of leading-edge carving in the design allows the entire planform to generate lift, and the final aircraft is both balanced and statically stable. This paper decomposes the aerodynamic forces into contributions from spanwise sections to explain how centerbody leading-edge carving can be used to create an efficient and stable BWB-type aircraft design.

A. Stability of Tailless Flying-Wing Aircraft

The flying wing and hybrid flying-wing aircraft configurations have been the subject of many studies since the late 1800s. These configurations are viewed by many as the most potentially efficient with regard to aerodynamics and structural weight. A historical account of the development of these configurations is given by Wood and Bauer [4]. Influential designs include the Junkers G-38 in 1931, the Horten Ho 229 in the early 1940s, the YB-49 in the late 1940s, and the Northrop Grumman B-2 developed in the 1980s.

Although the BWB is a hybrid flying wing because of its extended centerbody, its pitch stability and balance problems are similar to those found in swept flying-wing-type aircraft. For any aircraft, the net effect of the aerodynamic pressure forces on all the surfaces can be represented as a single, pure point force (with zero moment) at the center-of-pressure location. This is useful for examining balance and will be employed here where appropriate. Unfortunately, this representation is poorly suited for stability analyses, because the center of pressure moves in a complicated manner with the angle of attack.

A more effective approach is to represent the pressure forces by a point lift force at the fixed neutral point together with a constant moment about this neutral point. This then gives very simple criteria for positive pitch stability: the neutral point must be behind the center of gravity (c.g.) or, equivalently, the constant moment about the neutral point must be nose up. Because tailless flying-wing aircraft cannot rely on a downloaded tail to obtain this necessary nose-up pitching moment, two basic alternative approaches are used instead (sometimes in combination).

The first approach uses sweep together with washout twist, making the outer wings effectively act as a tail. But, with the strong wing tapers typical of jet transports, such a sweep-plus-twist combination would result in excessive unloading (or even negative loading) toward the tips, producing a loss of effective span and

Received 29 July 2009; revision received 28 October 2009; accepted for publication 5 December 2009. Copyright © 2010 by the authors. Published by the American Institute of Aeronautics and Astronautics, Inc., with permission. Copies of this paper may be made for personal or internal use, on condition that the copier pay the \$10.00 per-copy fee to the Copyright Clearance Center, Inc., 222 Rosewood Drive, Danvers, MA 01923; include the code 0021-8669/10 and \$10.00 in correspondence with the CCC.

^{*}Ph.D. Student, Engineering Department, Trumpington Street.

[†]Senior Lecturer, Engineering Department, Trumpington Street.

[‡]Lecturer, Engineering Department, Trumpington Street.

[§]Principal Research Engineer, Department of Aeronautics and Astronautics, 77 Massachusetts Avenue, Member AIAA.

^{||}Professor, Department of Aeronautics and Astronautics, 77 Massachusetts Avenue, Fellow AIAA.

^{**}Associate Professor, Department of Aeronautics and Astronautics, 77 Massachusetts Avenue, Member AIAA.

yielding an induced drag penalty. This penalty can be mitigated by increasing the tip chords, but this then increases the weight and the profile drag.

The alternative approach is to employ airfoils, which have a positive C_m (i.e., a nose-up moment) about their own neutral points (also called the aerodynamic centers), typically near the $c/4$ location. This mostly eliminates the need for washout twist and the associated induced drag penalty. Airfoils with positive C_m must generate most of their lift from the front of the airfoil. Unfortunately, this feature degrades transonic operation capability, which strongly favors aft loading and negative C_m .

B. Stability of the Blended-Wing Body

The problems associated with designing a balanced and stable tailless flying-wing aircraft using the methods described previously result from using airfoils with similar characteristics for the whole aircraft. Even with twist and sweep, the compromises needed result in a less than optimal performance. This was overcome with the BWB design (e.g., Liebeck [2]). BWB-type aircraft have a thick centerbody to carry passengers and cargo, and they use multiple airfoil profiles. The thick centerbody airfoil section used by Liebeck employs a reflex-cambered profile. The aircraft is balanced by downloading the rear of the centerbody (via reflex camber), where the centerbody now acts like a tail. Other BWB designs (for example, Qin et al. [3]) have also achieved longitudinal stability using this design feature. To help balance the aircraft, the lift distribution of the Liebeck [2] aircraft is triangular. This design compromises the results in increased lift-induced drag due to the nonelliptical lift distribution, but it must be noted that a triangular distribution also has some structural benefits.

II. Silent-Aircraft-Experimental-Design Aerodynamics

The SAX airframe design, developed under Hileman et al. [1], balances the pitch-down moment caused by the outer wings via a pitch-up moment from the centerbody. Rather than achieving this by downloading the rear of the aircraft, the SAX centerbody generates lift forward of the c.g. and, thus, a pitch-up moment, which is sufficient to balance the aircraft.

One of the intermediate designs, the SAX-29 (created during the course of SAI) was analyzed with a three-dimensional (3-D) Navier–Stokes computation. In addition to the 3-D Navier–Stokes analysis, SAX-29 was also examined using a 3-D panel method code (Newpan) and a two-dimensional (2-D) inviscid vortex lattice code (AVL) [1,5]. The breadth of analysis on the SAX-29 design will be exploited in this work. The conclusions that result should be applicable to any BWB-type of aircraft that uses leading-edge centerbody carving. The important aerodynamic characteristics of the SAX-29 at the beginning of cruise are detailed in Table 1.

The balancing of the SAX designs is illustrated in Fig. 1, which shows the local centers of pressure for the airfoils of the SAX-29. The centers of pressure for the centerbody airfoils are all ahead of the c.g. The aircraft is balanced by having the airfoil centers of pressure evenly distributed about the c.g. In this situation, the center of pressure is aligned with the c.g., as described by

$$\int_{\text{span}} c_l c (x_{cp} - x_{cg}) dy = 0 \quad (1)$$

Table 1 SAX-29 geometric and aerodynamic performance parameters

Parameter	Value
Wing area, m ²	845.5
Wing span, m	56.3
Reference chord length, m	15.0
Cruise Mach	0.8
Begin cruise altitude, ft	40,000
Begin cruise lift coefficient	0.194
Begin cruise angle of attack, deg	3.0

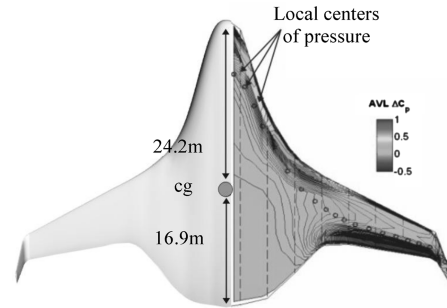


Fig. 1 Vortex lattice code (AVL) prediction showing wing loading, local centers of pressure, and the c.g. (Hileman et al. [1]).

where c_l is the local lift coefficient, c is the local chord, x_{cp} is the location of the local center of pressure, and x_{cg} is the location of the c.g.. All lengths are measured relative to the nose of the aircraft. Along with avoiding the inefficient downloading of the aircraft, generating lift at the nose is also a more natural location to balance moments about the c.g. This is because the c.g. of the SAX-29 is at 59% of the centerbody chord, as shown in Fig. 1. Consequently, the lever arm to generate moments about the c.g. is close to 50% larger for the nose (24.2 m) than it is for the rear of the centerbody (16.9 m), allowing larger moments to be generated for the same force. The outer wings can thus be efficiently designed, without any constraint on the pitching moment. This allows the use of conventional supercritical airfoils, which have high lift-to-drag ratios. The 3-D nature of the flow over the SAX-29 can be visualized via analysis of the inviscid streamlines. Figure 2 illustrates the strong transverse flows over the centerbody. As will be explored further in this section, this is a critical feature of BWB design.

A. Pressure Distributions on the SAX-29

The neutral point for an aircraft reflects the combined effects of the airfoils that comprise the aircraft. The airfoil equivalent of the neutral point will be referred to as the aerodynamic center in this paper.

There are two fundamentally different airfoils used in the SAX design: the centerbody airfoil and the outer-wing airfoil. Their cruise pressure distributions, at 78.6% of semispan and 7.1% of semispan, are presented in Fig. 3. The results are shown for angles of attack between 3.0 to 5.0 deg. The design configuration for the SAX-29 at the beginning of cruise is 3.0 deg, as shown in Table 1.

1. Outer Wings: Supercritical Airfoils

The outer-wing airfoil profile, depicted in Fig. 3, is similar to a modern supercritical wing. The airfoil has a 7% thickness-to-chord ratio, and the wing loading is distributed relatively evenly over the whole chord. For this reason, the center of pressure is close to the center of the airfoil. Additional lift is predominately generated over the front half of the airfoil, and so the aerodynamic center is near the quarter-point, as the thin airfoil theory would predict. The flow over the region is close to 2-D, as shown in the streamlines of Fig. 2, and so the thin airfoil theory can be applied over this region. Note that the center of pressure is behind the aerodynamic center (typical of modern airfoils), making the outer wings unstable about their centers of pressure. Further investigation of the aircraft design showed that the 7% thickness-to-chord ratio was too thin for practical application. Thus, thicker (8 to 9%) airfoils are suggested. This can be achieved without significant performance loss, as the maximum L/D of the outer airfoil is at a higher Mach number than the cruise speed.

2. Centerbody

Because of the 3-D nature of the flow, which is evident in Fig. 2, the pressure distribution over the centerbody changes in the spanwise direction. The pressure distribution shown in Fig. 3 is representative of most of the centerline. The majority of the lift is generated at the front of the airfoil, such that the rear of the airfoil is unloaded. The center of pressure for this airfoil is close to the nose, as shown in Fig. 1.

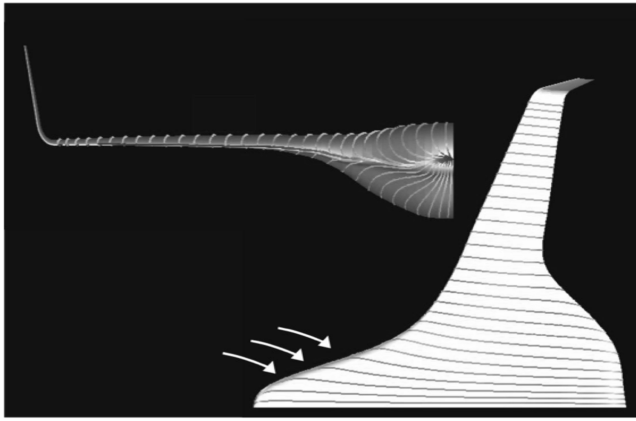


Fig. 2 Inviscid streamlines over SAX-29. Results from full-panel method code (Newpan).

The important result from Fig. 3 is that additional lift appears to be developing predominately over the center of the airfoil, indicating an aerodynamic center much further aft than the quarter-chord point. Calculations show that the aerodynamic center of the centerbody airfoil is at approximately 35% of the local chord. Thus, the center of pressure is ahead of the aerodynamic center, which makes the centerbody airfoil stable about its center of pressure.

B. Local c_l Values for SAX-29

The slopes of the local airfoil c_l values versus the angle of attack vary strongly across the span, as shown in Fig. 4. Over the outer wings, from 50–100% semispan, the $dc_l/d\alpha$ is close to constant, indicating that (as expected) the flow is 2-D. Over the centerbody, the $dc_l/d\alpha$ is greatly reduced, indicative of strong 3-D relief effects. This further illustrates that 2-D or strip-type methods cannot characterize the pitch stability characteristics of the overall BWB configuration, and 3-D methods are required.

C. Spanwise Lift Distribution for SAX-29

When compared with a conventional commercial aircraft, such as the Boeing 777, the SAX aircraft has an outer wing that is moderately loaded and a centerbody region that is lightly loaded. Using the loading from the beginning of cruise, and the estimating takeoff weight, the SAX-29 aircraft has an outer-wing loading of roughly

310 kg/m², whereas the centerbody loading is roughly 100 kg/m². These values are both below the Boeing 777 wing loading (takeoff weight normalized by lifting area) of roughly 570 kg/m². However, the resulting lift distribution is close to elliptical because of the differences in chord lengths between the centerbody and the outer wing. This can be observed in the spanwise lift distribution for the SAX-29 at 3.0 deg, as shown in Fig. 5.

D. Three-Dimensional Flow Features

A qualitative explanation of why the slopes ($\partial c_l / \partial \alpha$) in Fig. 4 are lower at locations that are close to the centerline, when compared with the outer wing, can be given with the aid of Fig. 6. The data show the 3-D Navier–Stokes calculation over the centerline along with a calculation using MSES, a 2-D compressible, viscous airfoil design and analysis tool [6].

The MSES calculation of Fig. 6 was conducted with the centerbody airfoil at cruise conditions, at the same local lift coefficient as in the 3-D case. The centerbody airfoil is relatively thick (14% t/c) when compared with traditional supercritical airfoils, and strong shocks are observed in the 2-D calculation at a cruise Mach of 0.8. The effect of 3-D pressure relief is large, such that the shocks on both the upper and lower surface disappear in the 3-D case.

The large region of high-velocity (and hence low pressure) flow over the upper surface of the aircraft, predicted via the 2-D code, does not occur on the 3-D aircraft. Instead, flow that is adjacent to the nose of the aircraft at ambient pressure is drawn in (as shown via the white arrows in Fig. 2), which reduces the region of low pressure. It appears that the 3-D effects over the centerbody reduce the ability of that region of the aircraft to carry a significant load. The effect is amplified

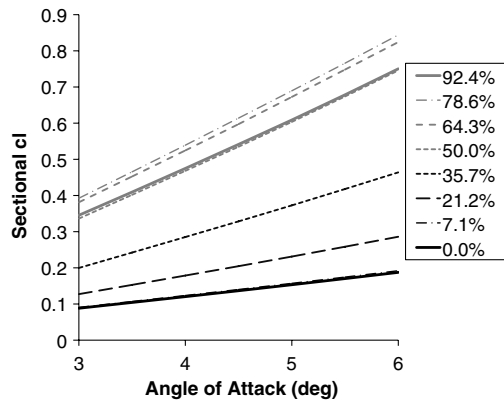


Fig. 4 Sectional lift coefficient given as a function of angle of attack. Legend provides sectional location as a percent of the aircraft semispan, $2y/b$. Results from 3-D Navier–Stokes solution.

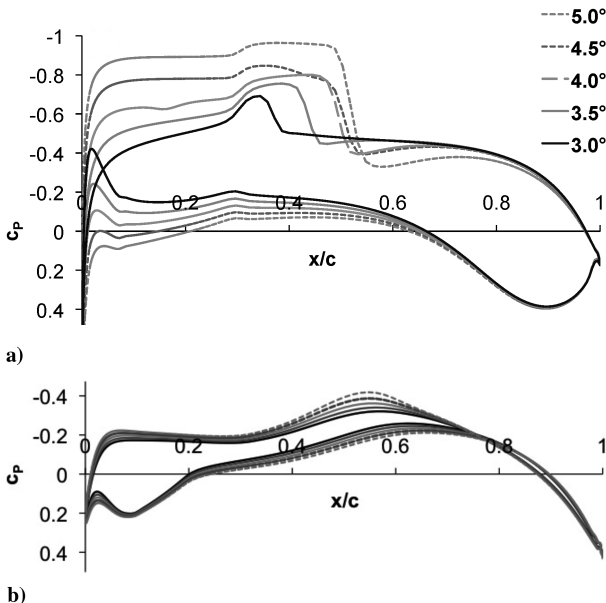


Fig. 3 Pressure distributions for various angles of attack α at a) 78.6% semispan and b) 7.1% semispan. Results from 3-D Navier–Stokes solution.

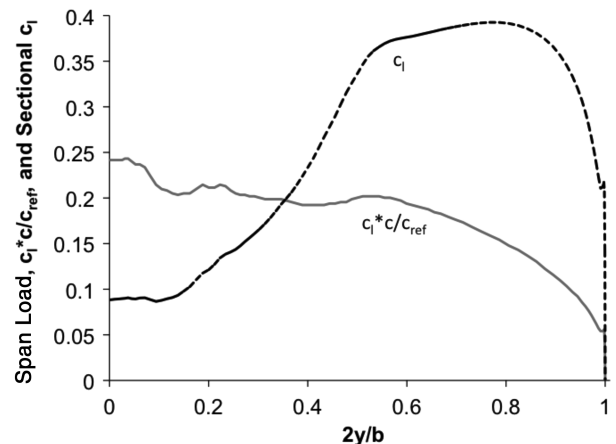


Fig. 5 Spanwise lift distribution, including sectional loading information. Results from 3-D Navier–Stokes solution.

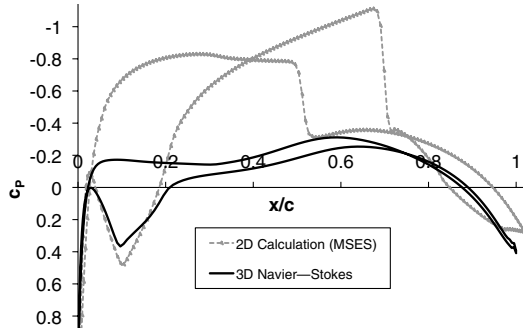


Fig. 6 Pressure distribution at 0.0% semispan (centerline).

at higher angles of attack, which results in a shallow c_l vs α curve for this region.

III. Section-Coefficient Analysis

The previous section has detailed some aerodynamic results from the SAX-29 aircraft. The results will now be analyzed in more depth by postprocessing the 3-D results in terms of local c_l and c_m coefficients. The sectional c_l vs α curves for the SAX-29 were shown in Fig. 4. The gradients ($\partial c_l / \partial \alpha$) as a function of span are shown in Fig. 7 for three flow solutions: a 3-D Navier–Stokes analysis, a full panel method code (Newpan), and a vortex lattice code (AVL).

The three codes show qualitative agreement. The difference at 100% semispan can be attributed to the winglet. The Navier–Stokes model did not incorporate the winglet, such that the loading drops off to zero at the wing tip. The Newpan and AVL models both incorporate the winglet, building a nonzero wing loading at 100% semispan. The AVL calculations for $\partial c_l / \partial \alpha$ closely match the 3-D Navier–Stokes calculations, which implies that the important features to be captured are the low-aspect-ratio planform and the correspondingly 3-D nature of the surrounding flow. The profiles of Fig. 7 are remarkably similar to the local sectional lift coefficients that were given in Fig. 5; that is, $\partial c_l / \partial \alpha \propto c_l(y)$. The ratio between them is shown in Fig. 8. The (approximate) relationship between $\partial c_l / \partial \alpha$ and $c_l(y)$ has implications for both induced drag and stability.

A. Induced Drag

The first implication from having $\partial c_l / \partial \alpha \propto c_l(y)$ is that, because additional lift is proportional to the local lift coefficient, the aircraft maintains a lift distribution that is close to elliptical over a large range of angles of attack, as can be observed from the data in Fig. 9. Figure 9 is identical to Fig. 5, except the spanwise lift distribution is shown for a range of angles of attack. As the angle of attack increases, the spanwise lift distribution stays close to elliptical.

If $\partial c_l / \partial \alpha$ is constant, then obtaining an elliptic lift distribution over a large range of angles of attack is only possible with a planform distribution that is, itself, elliptical. Because $\partial c_l / \partial \alpha \propto c_l(y)$, the induced drag for the SAX is low over a large range of angles of attack.

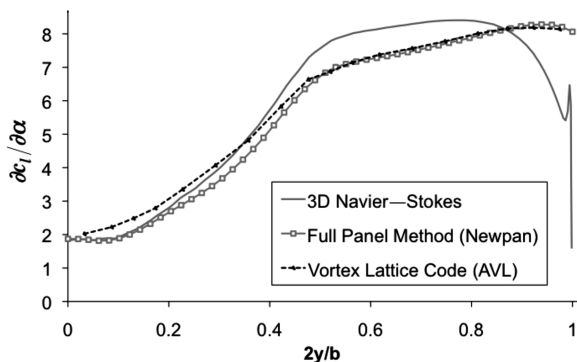


Fig. 7 Comparison of spanwise $\partial c_l / \partial \alpha$ among three simulations.

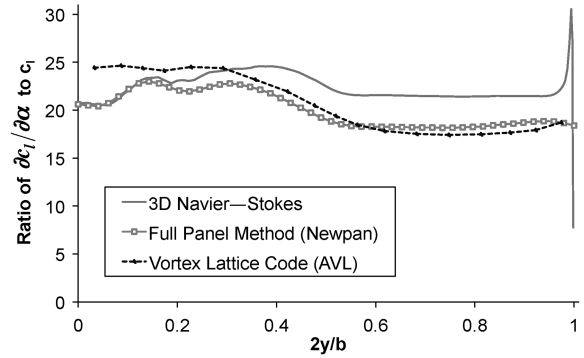


Fig. 8 Comparison of spanwise ratio between $\partial c_l / \partial \alpha$ and c_l among three simulations.

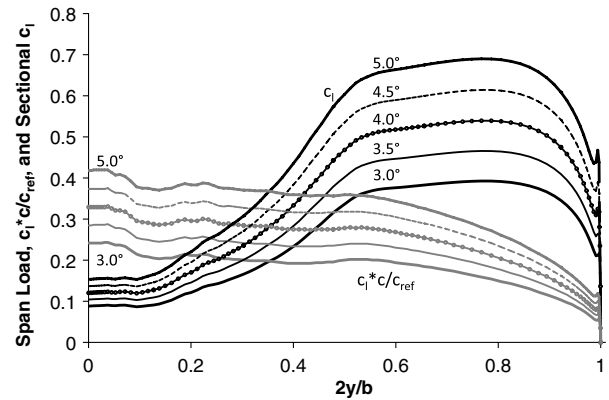


Fig. 9 Spanwise loading and lift distribution for angles of attack between 3 and 5 deg, in 0.5 deg increments. Results from 3-D Navier–Stokes solution.

B. Stability

The similarity in behavior of the slope of $\partial c_l / \partial \alpha$ and the sectional lift coefficient $c_l(y)$ has a profound impact on tailless aircraft stability. This can be shown via examination of the stability condition, as defined in Eq. (2):

$$\int_{\text{span}} \frac{dc_l}{d\alpha} c(x_{ac} - x_{cg}) dy > 0 \quad (2)$$

Recall that the locations of the airfoils' aerodynamic centers and the global c.g. are measured from the nose of the aircraft. Equation (2) states that the aircraft neutral point needs to be aft of the aircraft c.g. to stabilize the aircraft.

If $\partial c_l / \partial \alpha \propto c_l(y)$, as it appears for a BWB-type configuration that uses centerbody leading-edge carving (such as the SAX-29 and the SAX-40), the stability equation reduces to

$$\int_{\text{span}} c_l c(x_{ac} - x_{cg}) dy > 0 \quad (3)$$

Equation (4) implies that the aircraft neutral point is found in the same way as the aircraft center of pressure; that is, the neutral point is weighted by the lift each airfoil is carrying. So the neutral point is weighted by both the airfoil chord and the local lift coefficient. Because the centerbody has a low c_l and the outer wings have a high c_l , this weights the neutral point further toward the rear of the aircraft, making it easier to balance, because it allows the c.g. and the center of pressure to align at a location further aft on the planform. If the aircraft is designed to be balanced, as described by Eq. (1), then Eq. (3) simplifies to Eq. (4):

$$\begin{aligned}
& \int_{\text{span}} c_l c(x_{ac} - x_{cg}) dy \\
&= \int_{\text{span}} c_l c(x_{ac} - x_{cp}) dy + \int_{\text{span}} c_l c(x_{cp} - x_{cg}) dy \\
&\rightarrow \int_{\text{span}} c_l c(x_{ac} - x_{cp}) dy > 0 \quad (4)
\end{aligned}$$

Equation (4) implies that, if a BWB-type aircraft is to be designed to be balanced with leading-edge carving of the centerbody (instead of centerbody downloading with reflex-cambered airfoils), centerbody airfoils are needed with local aerodynamic centers behind their local centers of pressures, in proportion to the generated lift. For example, if half the total lift is generated by supercritical airfoils that have aerodynamic centers that are, on average, X m ahead of their local centers of pressures, the centerbody airfoils must not only generate the remaining lift, but they must do so with aerodynamic centers that are, on average, more than X m behind their respective local centers of pressure. Equation (4) also implies that an aircraft similar to SAX can never be balanced by only using airfoils that have aerodynamic centers ahead of their local centers of pressure. This is because, by continuation, the aircraft neutral point would be ahead of the c.g.

C. Design Implications

The local centers of pressure, normalized by the local airfoil chord lengths, are shown for the SAX-29 in Fig. 10. Many important aspects are shown in this figure. First, lift is generated toward the front of the centerbody airfoils and toward the rear of the outer-wing airfoils, as shown in Fig. 3. Second, as shown by the aerodynamic center data from Fig. 3, the aerodynamic centers of the centerbody and outer-wing sections are behind and forward of the local centers of pressure, respectively. This can be further observed from the centers of pressure for the centerbody airfoils moving back with increasing angles of attack, indicative of an aerodynamic center behind the center of pressure. Conversely, the centers of pressure for the outer wings move forward, indicative of local aerodynamic centers that are ahead of the centers of pressure.

Equation (4) can be used with the information contained within Figs. 9 and 10 to define the centerbody properties that are necessary to create a balanced and statically stable BWB-type aircraft. To demonstrate this, the integral in Eq. (4) has been broadly divided into a summation for the outer wing and a summation for the centerbody regions, as shown in Eq. (5),

$$c_{l,C} S_C (x_{ac} - x_{cp})_C + c_{l,O} S_O (x_{ac} - x_{cp})_O > 0 \quad (5)$$

where the subscripts C and O denote summation over the centerbody and outer wing, respectively. This relationship can be rearranged to solve for the centerbody airfoil properties, as shown in Eq. (6):

$$(x_{ac} - x_{cp})_C > \frac{c_{l,O} S_O (x_{cp} - x_{ac})_O}{c_{l,C} S_C} \quad (6)$$

The cross section dividing the centerbody and the outer wing was chosen to correspond to where the sectional airfoil aerodynamic center matches the sectional center of pressure, $2y/b = 0.31$. Using this delineation, the quantities within Eq. (6) were computed from the aircraft geometry and the data contained in Figs. 9 and 10. The result is that the value of $(x_{ac} - x_{cp})_C$ needs to be greater than 3.1 m (i.e., the average aerodynamic center of the centerbody region needs to be over 3.1 m aft of the average center of pressure of the centerbody region). As mentioned, the aerodynamic center of the centerbody (at $2y/b = 0.071$) was calculated to be at 35.4% of the local chord, which is almost 6.5 m aft of the local center of pressure at an angle of attack of $\alpha = 3$ deg. This difference is crucial in enabling the SAX design to be stable.

IV. Conclusions

By incorporating centerbody leading-edge carving into the aerodynamic design of an airframe, a BWB-type aircraft can be both balanced and made statically stable, without the need for downloading any part of the aircraft. Furthermore, the outer wings

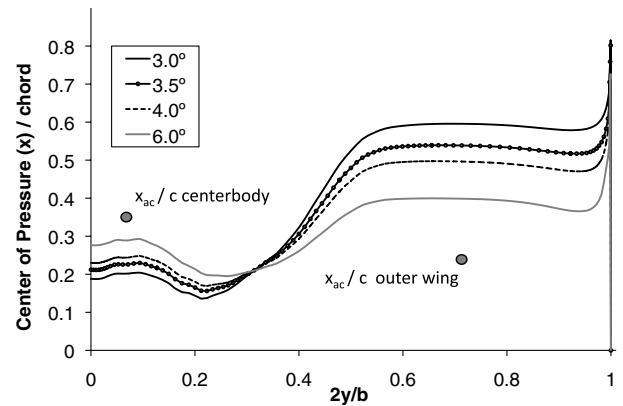


Fig. 10 Spanwise distribution of normalized local centers of pressure, with aerodynamic centers for airfoil sections on the centerbody and outer wing. Results from 3-D Navier–Stokes solution.

can be optimized for aerodynamic efficiency, without any constraint on the pitching moment, because the pitching moment can be effectively balanced via the centerbody. Through decomposition of the aerodynamic forces, the unique benefits of centerbody leading-edge carving can be quantified, and a design guideline can be established to determine the amount of leading-edge carving that is necessary for aircraft stability. The analysis shows that lift needs to be developed approximately equally by airfoils that are stable about their centers of pressure and airfoils that are unstable about their centers of pressure. Because modern supercritical airfoils (which are unstable about their centers of pressure) are the natural choice for the outer wings due to their improved transonic performance, this requires that stable airfoils are required for the design of the centerbody. The effect of centerbody leading-edge carving has other benefits. It allows the induced drag to remain low over a range of lift coefficients by maintaining a lift distribution that is close to elliptical. The combined effect of an elliptical lift distribution and the use of supercritical airfoils results in an aircraft design with improved aerodynamic performance when compared with traditional BWB-type aircraft.

Acknowledgments

This research was funded by the Cambridge–MIT Institute, which is gratefully acknowledged. Matthew Sargeant is grateful to the Cambridge Australia Trust for his doctoral fellowship. The authors graciously acknowledge the invaluable assistance of Dino Roman, Bob Liebeck, and Sean Wakayama from the Boeing Phantom Works. All three-dimensional Navier–Stokes calculations were performed by Dino Roman at the Boeing Phantom Works. The authors are also indebted to many members of the Silent Aircraft Initiative who have been instrumental to the silent aircraft project.

References

- [1] Hileman, J. I., Spakovszky, Z. S., Drela, M., Sargeant, M., and Jones, A., "Airframe Design for Silent Fuel-Efficient Aircraft," *Journal of Aircraft*, Vol. 47, No. 3, 2010, pp. 956–969.
- [2] Liebeck, R. L., "Design of the Blended-Wing–Body Subsonic Transport," *Journal of Aircraft*, Vol. 41, No. 1, 2004, pp. 10–25. doi:10.2514/1.9084
- [3] Qin, N., Vavalle, A., Le Moigne, A., Laban, M., Hackett, K., and Weinerfelt, P., "Aerodynamic Considerations of Blended-Wing–Body Aircraft," *Progress in Aerospace Sciences*, Vol. 40, No. 6, 2004, pp. 321–343. doi:10.1016/j.paerosci.2004.08.001
- [4] Wood, R. M., and Bauer, X. S., "Flying Wings/Flying Fuselages," AIAA Paper 2001-311, 2001.
- [5] Drela, M., and Youngren, H., "AVL Overview" [online product brochure], <http://web.mit.edu/drela/Public/web/avl/> [retrieved Oct. 2004].
- [6] Drela, M., "MSES Multi-Element Airfoil Design/Analysis Software: Summary" [online product brochure], March 2004, <http://raphael.mit.edu/drela/mssesum.ps> [retrieved 12 Nov. 2005].